

## MIT Open Access Articles

*Identification and Rescue of  $\alpha$ -Synuclein Toxicity in Parkinson Patient-Derived Neurons*

The MIT Faculty has made this article openly available. **Please share** how this access benefits you. Your story matters.

**Citation:** Chung, Chee Yeun, Vikram Khurana, Pavan K. Auluck, Daniel F. Tardiff, Joseph R. Mazzulli, Frank Soldner, Valeriya Baru, et al. "Identification and Rescue of  $\alpha$ -Synuclein Toxicity in Parkinson Patient-Derived Neurons." *Science* 342, no. 6161 (October 24, 2013): 983–987.

**As Published:** <http://dx.doi.org/10.1126/science.1245296>

**Publisher:** American Association for the Advancement of Science (AAAS)

**Persistent URL:** <http://hdl.handle.net/1721.1/92886>

**Version:** Author's final manuscript: final author's manuscript post peer review, without publisher's formatting or copy editing

**Terms of Use:** Article is made available in accordance with the publisher's policy and may be subject to US copyright law. Please refer to the publisher's site for terms of use.





Published as: *Science*. 2013 November 22; 342(6161): 983–987.

## Identification and Rescue of $\alpha$ -Synuclein Toxicity in Parkinson Patient-Derived Neurons

Chee Yeun Chung<sup>1,†</sup>, Vikram Khurana<sup>1,2,†</sup>, Pavan K. Auluck<sup>1,3</sup>, Daniel F. Tardiff<sup>1</sup>, Joseph R. Mazzulli<sup>2</sup>, Frank Soldner<sup>1</sup>, Valeriya Baru<sup>1,4</sup>, Yali Lou<sup>1,4</sup>, Yelena Freyzon<sup>1</sup>, Sukhee Cho<sup>5</sup>, Alison E. Mungenast<sup>5</sup>, Julien Muffat<sup>1</sup>, Maisam Mitalipova<sup>1</sup>, Michael D Pluth<sup>6</sup>, Nathan T. Jui<sup>6</sup>, Birgitt Schüle<sup>7</sup>, Stephen J. Lippard<sup>6</sup>, Li-Huei Tsai<sup>5,8</sup>, Dimitri Krainc<sup>2</sup>, Stephen L. Buchwald<sup>6</sup>, Rudolf Jaenisch<sup>1,8</sup>, and Susan Lindquist<sup>1,4,9,\*</sup>

<sup>1</sup>Whitehead Institute for Biomedical Research, Cambridge, MA 02142, USA

<sup>2</sup>Department of Neurology, Massachusetts General Hospital and Harvard Medical School, Boston, MA 02114, USA

<sup>3</sup>Department of Pathology (Neuropathology), Massachusetts General Hospital and Harvard Medical School, Boston, MA 02114, USA

<sup>4</sup>Howard Hughes Medical Institute, Department of Biology, Massachusetts Institute of Technology, Cambridge, MA

<sup>5</sup>The Picower Institute for Learning and Memory, Department of Brain and Cognitive Sciences, Massachusetts Institute of Technology, Cambridge, MA 02139, USA

<sup>6</sup>Department of Chemistry, Massachusetts Institute of Technology, Cambridge, MA 02139, USA

<sup>7</sup>The Parkinson's Institute, Sunnyvale, CA 94085

<sup>8</sup>Howard Hughes Medical Institute, Cambridge, MA

<sup>9</sup>Department of Biology, Massachusetts Institute of Technology, Cambridge, MA

### Abstract

The induced pluripotent stem (iPS) cell field promises a new era for *in vitro* disease modeling. However, identifying innate cellular pathologies, particularly for age-related neurodegenerative

\*Correspondence to: Dr Susan Lindquist, lindquist\_admin@wi.mit.edu.

†These authors contributed equally to this work and are listed alphabetically.

Supplementary Materials

[www.sciencemag.org](http://www.sciencemag.org)

Materials and Methods

Figures S1–S10

Table S1

References (29–40) [Note: The numbers refer to any additional references cited only within the Supplementary Materials]

**Author contributions:** CYC, VK and SL conceptualized the study, designed the experiments, and wrote the paper. VK developed the human IPS cell-derived cortical synucleinopathy model, assisted by YL. Pluripotent cell lines, advice on experimental design or technical expertise were provided by FS, JRM, JM, MM and RJ. FS reprogrammed the WIBR-IPS-SYN<sup>TRPL</sup> line from fibroblasts provided by BS. CYC developed the rat cortical synucleinopathy model, assisted by LB. The mKate2-tagged constructs were generated by YF. CYC and VK performed all experiments except: fig. 1D and E, fig. 2E, fig. S5A and B (PKA); fig. 4A (DFT); fig. 4C, fig. S6C (JRM/DK); fig. S2, H–I (AEM/SC/LT); fig. S1 (YF/YL). The small molecule NAB2 was synthesized by NTJ and SLB, based on a yeast screen performed by DFT. FL2 dye synthesis and technical advice were provided by MDP and SJL. CYC, VK and SL are inventors on a pending patent application related to work described in this paper.

diseases, has been challenging. Here, we exploited mutation correction of iPS cells and conserved proteotoxic mechanisms from yeast to human to discover and reverse phenotypic responses to  $\alpha$ -Synuclein ( $\alpha$ Syn), a key protein involved in Parkinson's disease (PD). We generated cortical neurons from iPS cells of patients harboring  $\alpha$ Syn mutations, who are at high risk of developing PD dementia. Genetic modifiers from unbiased screens in a yeast model of  $\alpha$ Syn toxicity led to identification of early pathogenic phenotypes in patient neurons. These included nitrosative stress, accumulation of ER-associated degradation (ERAD) substrates and ER stress. A small molecule identified in a yeast screen, and the ubiquitin ligase Nedd4 it activates, reversed pathologic phenotypes in these neurons.

---

Neurodegenerative dementias are devastating and incurable diseases for which we desperately need tractable cellular models to investigate pathologies and discover therapeutics. Parkinson disease dementia (PDD) is a major debilitating non-motor manifestation of Parkinson's disease, affecting as many as 80% of patients (1). The best pathologic correlate of PDD is neuron loss and pathologic aggregation of  $\alpha$ Syn within deep layers of the cerebral cortex (1). Contursi kindred patients, who harbor an autosomal dominant and highly penetrant A53T mutation in  $\alpha$ Syn, manifest prominent PD and dementia (2, 3). iPS cells from a female member of this kindred (Table S1) have recently been mutation-corrected to control for genetic background effects (4). To establish a model for cortical synucleinopathy, we differentiated two pairs of subclones from these lines (fig. S1) into cortical neurons (fig. S2 and S3).

Over 12 weeks of differentiation, cultures consisted primarily of excitatory glutamatergic neurons mixed with glia (fig. S2, C to E; fig. S3). To identify neurons, neural precursors were infected prior to differentiation with lentiviruses expressing enhanced yellow fluorescent protein (eYFP) or red fluorescent protein (RFP) under the control of the synapsin promoter (fig. S2G). When co-cultured, A53T and corrected neurons were electrically active at 8 weeks of differentiation. They exhibited similar calcium fluxes and electrophysiology (fig. S2, H and I). The majority of neurons were immunopositive for Tbr1, a transcription factor indicating developing deep cortical layers (fig. S2E) (5).  $\alpha$ Syn was robustly expressed, but only after neuronal differentiation (fig. S2, C to F).  $\alpha$ Syn was both cytoplasmic and punctate in neuronal processes (fig. S2, C to E). Thus, these cells provide a relevant substrate for examining early  $\alpha$ Syn-related cortical pathologies.

It has been difficult to establish neurodegenerative phenotypes in iPS cell-derived neurons that can be solely attributable to disease-causing genetic mutations. Previous studies accelerated degenerative phenotypes with toxins such as oxidative stressors (6–8). In addition, inconsistent differentiation precludes these cells from being used in high-throughput screening. To address these problems, we turned to a yeast platform in which  $\alpha$ Syn-expression results in toxicity (9, 10) and disease-relevant phenotypes, including focal accumulation of  $\alpha$ Syn, mitochondrial dysfunction,  $\alpha$ Syn-mediated vesicle trafficking defects, links to genetic and environmental risk factors, and sensitivity to  $\alpha$ Syn dosage (9–12). We reasoned that unbiased genetic analysis in this system could guide discovery of innate pathologic phenotypes.

Previous unbiased yeast genetic screens, encompassing 85% of the yeast proteome, identified robust modifiers of  $\alpha$ Syn toxicity (9, 12). We first tested Fzf1, a transcriptional regulator of nitrosative stress responses (13) that suppressed  $\alpha$ Syn toxicity in yeast (fig. 1A). Nitrosative stress is caused by nitric oxide (NO) and related redox forms. Though it is not known if there is a direct causal connection between nitrosative stress and  $\alpha$ Syn toxicity, the nitration of tyrosine residues is increased in postmortem brain from synucleinopathy patients (14, 15).

To determine if nitrative damage occurs to yeast proteins in direct response to  $\alpha$ Syn, we took advantage of an antibody to nitrotyrosine. In yeast, this antibody exhibited minimal background in control strains, allowing us to detect intense protein nitration that was tightly dependent on  $\alpha$ Syn dosage (fig. 1B). Importantly, nitration was a highly specific response to  $\alpha$ Syn toxicity and was not observed with other neurodegenerative disease proteins expressed at equally toxic levels, including Abeta peptide, TDP-43, polyQ-expanded huntingtin and Fus (fig. 1B).

Fzf1 expression strongly decreased protein nitration induced by  $\alpha$ Syn (fig. 1C). Next, we asked if  $\alpha$ Syn toxicity could be tuned by altering the production of NO. In yeast, NO levels are regulated by switching between distinct isoforms of mitochondrial cytochrome *c* oxidase (COX5): deletion of COX5A increases NO; deletion of COX5B decreases it (16). Indeed, these manipulations increased and decreased nitrotyrosine levels in response to  $\alpha$ Syn (fig. 1D). Toxicity increased and decreased commensurately (fig. 1E). Thus, in yeast, nitrosative stress is not simply a consequence of  $\alpha$ Syn toxicity, but contributes to toxicity.

To investigate a connection between  $\alpha$ Syn and nitrosative stress in neurons we employed FL2, a copper and fluorescein-based NO sensor (17). We optimized the use of FL2 with rat primary cortical cultures (fig. S4), a neuronal synucleinopathy model.  $\alpha$ Syn overexpression increased the FL2 signal, with a perinuclear distribution in the cell body (fig. 2A) that partially co-localized with the endoplasmic reticulum (ER; fig. 2B). High density of processes and mixed cell types hindered intensity measurements outside well-defined neuronal cell bodies.

Having optimized the FL2 assay in rat neurons, we turned to our Parkinson patient-derived cortical neurons at 8 weeks of differentiation. Two isogenic pairs of A53T and mutation-corrected neurons were differentiated in parallel and labeled with synapsin-RFP (see fig. S2G). Intraneuronal FL2 signals increased in A53T neurons relative to corrected neurons, again most readily visualized in the cell body. As in rodent neurons, there was partial co-localization of this signal with an ER marker (fig. 2C). Cytoplasmic nitrotyrosine staining also accumulated in mutant neurons compared to corrected neurons (fig. 2D). Similarly, cytoplasmic nitrotyrosine staining was prominent in neurons and neuropil of post-mortem frontal cortex from another subject in the same kindred (18), but not in control brain (fig. 2E).

The yeast synucleinopathy model exhibits ER stress, ER-associated degradation (ERAD) substrate accumulation and defective trafficking from the ER to Golgi (12). ER stress has also been described in a mouse synucleinopathy model (19). Because NO was visualized in

the vicinity of the ER in neurons (fig. 2), we asked whether modulating NO levels modulates ER stress. Indeed, manipulating COX5 isoforms, to increase and decrease NO levels, commensurately altered the unfolded protein response (fig. S5A) and the ER accumulation of carboxypeptidase Y (CPY; S5B), a well-characterized ERAD substrate that traffics between the ER and vacuole (12). This required the presence of  $\alpha$ Syn (fig. S5), implying a connection between nitrosative and ER stress in the context of  $\alpha$ Syn toxicity. Correspondingly, two hallmarks of ER stress – PDI (protein disulfide isomerase) and BIP (binding immunoglobulin protein) – increased at 12 weeks of differentiation in the A53T neurons compared to corrected cells. Levels of CHOP (CCAAT enhancer-binding protein homologous protein), a component of ER stress-induced apoptosis, did not change, indicating cellular pathology was still at an early-stage (fig S5C).

Next, we assessed the accumulation and trafficking of three ERAD substrates implicated in neurodegeneration: Glucocerebrosidase (GCase), Neuroserpin and Nicastrin (20). GCase mutations are common risk factors for PD and confer risk for cognitive impairment in this disease (21). GCase accumulates in the ER of cultured cells over-expressing  $\alpha$ Syn (22). ER forms of GCase and Nicastrin accumulated, and the ratio of post ER/ER forms declined in A53T compared to mutation-corrected patient neurons starting at four weeks (fig. 3, A and B; fig. S, 6A to C). Neuroserpin was not affected at the timepoints we examined (fig. 3, A and B; fig. S6, A to C). Levels of neuron-specific markers were unaffected (fig. 3C and fig. S6C). These findings were consistent in multiple rounds of differentiation, robust to distinct differentiation protocols (fig. S6C). Phenotypes were not present in the undifferentiated iPS cell lines (fig. S6D). Thus, ERAD dysfunction is an early and progressive cellular phenotype in response to mutated  $\alpha$ -Syn in patient neurons.

The increase in the ER form of GCase, and the decrease in the post-ER to ER ratio, was recapitulated in the brain of an A53T patient (fig. 3C and fig. S7B). Cortex from sporadic PD samples exhibited the same trend (fig. S7). We also analyzed cortical neurons generated from the iPS cells of a male patient of the “Iowa kindred”. This patient harbored a triplication of the wild-type  $\alpha$ Syn gene and manifested aggressive dementia in addition to parkinsonism (Table S1). Aged cortical neurons generated from a male human embryonic stem cell line BG01(23) served as a control. ERAD substrates accumulated (fig. 3A and fig. S6B) and ER stress increased (fig. S5C) in neurons from this patient, closely phenocopying A53T cells.

Another suppressor of  $\alpha$ Syn toxicity recovered in the yeast screen was Hrd1 (fig. 3D, left) (9). Hrd1 is a highly conserved E3 ubiquitin ligase (Synoviolin-1 or Syvn1 in humans) that plays a critical role in ERAD from yeast to human. In primary rat cortical neurons lentiviral expression of Syvn1 rescued  $\alpha$ Syn toxicity in a dose-dependent manner (fig. 3D, right). Syvn1 also reduced nicastrin and GCase accumulation in the ER of the A53T patient cortical neurons (fig. 3E).

Next, we tested the ability of NAB2 (24) to rescue the pathological phenotypes we discovered here in both yeast cells and PD neurons. NAB2, an N-arylbenzimidazole, was recovered in a yeast screen of more than 180,000 small molecules and rescues  $\alpha$ Syn toxicity in yeast by activating the Rsp5/Nedd4 pathway (24). This protein is another highly

conserved ubiquitin ligase, and plays a key role in regulating vesicle trafficking (25, 26). NAB2 reduced protein nitration in the yeast syucleinopathy model (fig. 4A) and decreased NO levels in A53T patient neurons (fig. 4B). Moreover, NAB2 reduced the accumulation of immature ER forms of CPY in yeast (fig. 4A). It increased the post-ER forms, and decreased the immature forms, of Nicastrin and GCase in PD patient neurons (fig. 4C and fig. S8). Furthermore, NAB2 analogs that were inactive in yeast (24) were also inactive in human neurons (fig. S9). Connecting NAB2 back to the ubiquitin ligase, we used a lentivirus to overexpress Nedd4. This phenocopied the effects of the compound, increasing the mature forms of Nicastrin and GCase (fig. 4D).

Conserved biology in a cross-species cellular discovery platform, as described here enabled the discovery of innate pathologic phenotypes in neurons derived from patients with PD. It also enabled the identification of genes and small molecules that reverted these phenotypes (24) (fig. S10). A similar approach might be useful in the study of other PD-relevant phenotypes identified in yeast, including mitochondrial dysfunction and perturbed metal ion homeostasis (9,11). The existence of other yeast models of neurodegenerative diseases suggest that this approach will be generalizable to other diseases (11, 27, 28).

## Supplementary Material

Refer to Web version on PubMed Central for supplementary material.

## Acknowledgments

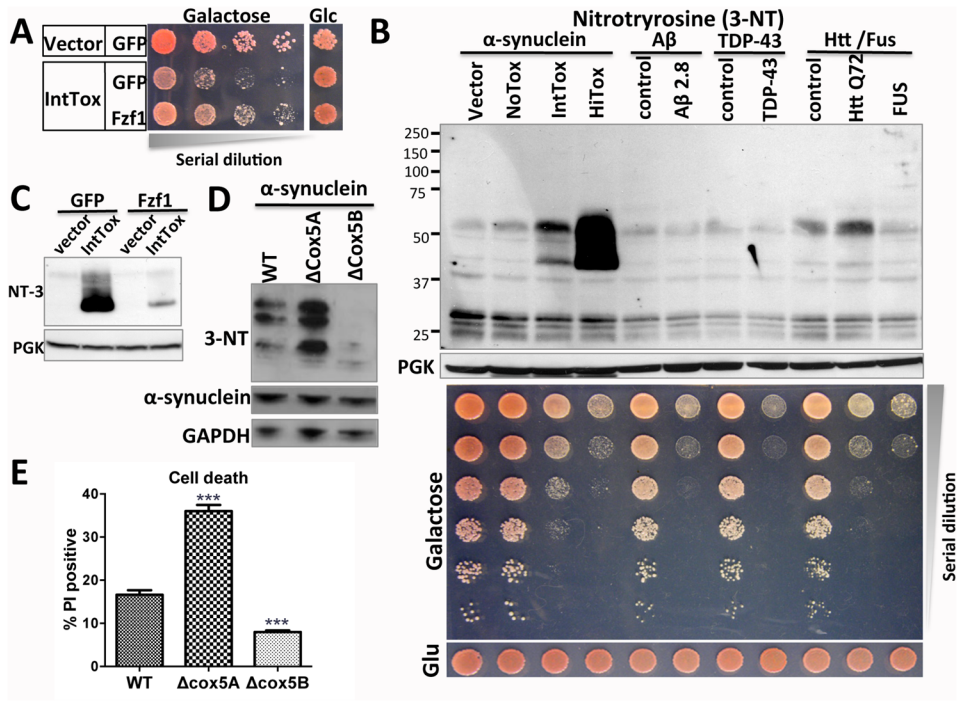
We thank Dennis Dickson, Larry Golbe and John Trojanowki for postmortem tissue or data; David Pincus for the UPR reporter; Jan Pruszek, Patti Wisniewski, Iain Cheeseman for giving important technical advice; Raaji Alagappan, Tenzin Lungiangwa and Ping Xu for superb technical assistance; Sandro Santagata, Luke Whitesell, Mel Feany, Dirk Landgraf and Linda Clayton for fruitful discussion and critical comments on the manuscript. Grant support was provided by a Howard Hughes Medical Institute Collaborative Innovation Award (SL), JPB Foundation grants (SL), NIH/NIA K01 AG038546 (CYC), American Brain Foundation and Parkinson's Disease Foundation Clinician-Scientist Development Award (VK), NIH 5 R01CA084198 (RJ), JBP foundation (LHT) and NSF (SJL).

## References

1. Irwin DJ, et al. Neuropathologic substrates of Parkinson disease dementia. *Ann Neurol.* 2012; 72:587–598. [PubMed: 23037886]
2. Spira PJ, Sharpe DM, Halliday G, Cavanagh J, Nicholson GA. Clinical and pathological features of a Parkinsonian syndrome in a family with an Ala53Thr alpha-synuclein mutation. *Ann Neurol.* 2001; 49:313–319. [PubMed: 11261505]
3. Markopoulou K, et al. Clinical, neuropathological and genotypic variability in SNCA A53T familial Parkinson's disease. Variability in familial Parkinson's disease. *Acta Neuropathol.* 2008; 116:25–35. [PubMed: 18389263]
4. Soldner F, et al. Generation of isogenic pluripotent stem cells differing exclusively at two early onset Parkinson point mutations. *Cell.* 2011; 146:318–331. [PubMed: 21757228]
5. Saito T, et al. Neocortical Layer Formation of Human Developing Brains and Lissencephalies: Consideration of Layer-Specific Marker Expression. *Cerebral Cortex.* 2011; 21:588–596. [PubMed: 20624841]
6. Nguyen HN, et al. LRRK2 mutant iPSC-derived DA neurons demonstrate increased susceptibility to oxidative stress. *Cell stem cell.* 2011; 8:267–280. [PubMed: 21362567]

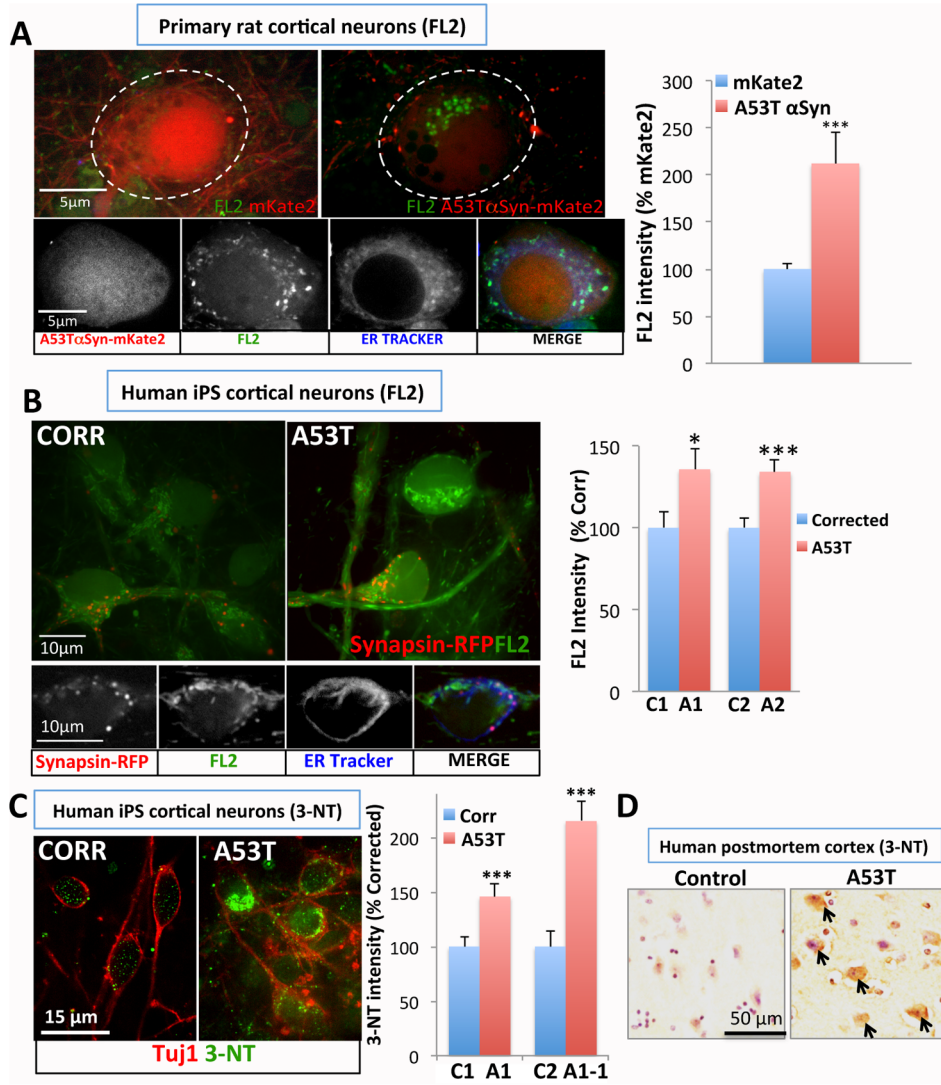
7. Byers B, et al. SNCA Triplication Parkinson's Patient's iPSC-derived DA Neurons Accumulate  $\alpha$ -Synuclein and Are Susceptible to Oxidative Stress. *PLoS ONE*. 2011; 6:e26159. [PubMed: 22110584]
8. Cooper O, et al. Pharmacological rescue of mitochondrial deficits in iPSC-derived neural cells from patients with familial Parkinson's disease. *Sci Transl Med*. 2012; 4:141ra90.
9. Gitler AD, et al. Alpha-synuclein is part of a diverse and highly conserved interaction network that includes PARK9 and manganese toxicity. *Nat Genet*. 2009; 41:308–315. [PubMed: 19182805]
10. Outeiro TF, Lindquist S. Yeast cells provide insight into alpha-synuclein biology and pathobiology. *Science*. 2003; 302:1772–1775. [PubMed: 14657500]
11. Khurana V, Lindquist S. Modelling neurodegeneration in *Saccharomyces cerevisiae*: why cook with baker's yeast? *Nat Rev Neurosci*. 2010; 11:436–449. [PubMed: 20424620]
12. Cooper AA, et al. Alpha-synuclein blocks ER-Golgi traffic and Rab1 rescues neuron loss in Parkinson's models. *Science*. 2006; 313:324–328. [PubMed: 16794039]
13. Sarver A, DeRisi J. Fzf1p regulates an inducible response to nitrosative stress in *Saccharomyces cerevisiae*. *Mol Biol Cell*. 2005; 16:4781–4791. [PubMed: 16014606]
14. Giasson BI, et al. Oxidative damage linked to neurodegeneration by selective alpha-synuclein nitration in synucleinopathy lesions. *Science*. 2000; 290:985–989. [PubMed: 11062131]
15. Gómez-Tortosa E, et al. Patterns of protein nitration in dementia with Lewy bodies and striatonigral degeneration. *Acta Neuropathol*. 2002; 103:495–500. [PubMed: 11935266]
16. Castello PR, et al. Oxygen-regulated isoforms of cytochrome c oxidase have differential effects on its nitric oxide production and on hypoxic signaling. *Proc Natl Acad Sci USA*. 2008; 105:8203–8208. [PubMed: 18388202]
17. Pluth MD, Tomat E, Lippard SJ. Biochemistry of Mobile Zinc and Nitric Oxide Revealed by Fluorescent Sensors. *Annu Rev Biochem*. 2011; 80:333–355. [PubMed: 21675918]
18. Kotzbauer PT, et al. Fibrillization of alpha-synuclein and tau in familial Parkinson's disease caused by the A53T alpha-synuclein mutation. *Exp Neurol*. 2004; 187:279–288. [PubMed: 15144854]
19. Colla E, et al. Endoplasmic reticulum stress is important for the manifestations of  $\alpha$ -synucleinopathy in vivo. *J Neurosci*. 2012; 32:3306–3320. [PubMed: 22399753]
20. Tabuchi K, Chen G, Südhof TC, Shen J. Conditional forebrain inactivation of nicastrin causes progressive memory impairment and age-related neurodegeneration. *J Neurosci*. 2009; 29:7290–7301. [PubMed: 19494151]
21. Alcalay RN, et al. Cognitive performance of GBA mutation carriers with early-onset PD: the CORE-PD study. *Neurology*. 2012; 78:1434–1440. [PubMed: 22442429]
22. Mazzulli JR, et al. Gaucher disease glucocerebrosidase and  $\alpha$ -synuclein form a bidirectional pathogenic loop in synucleinopathies. *Cell*. 2011; 146:37–52. [PubMed: 21700325]
23. Mitalipova M, et al. Human embryonic stem cell lines derived from discarded embryos. *STEM CELLS*. 2003; 21:521–526. [PubMed: 12968106]
24. Tardiff DF, et al. Phenotypic screening and chemical genetics reveals a “druggable” Rsp5/Nedd4 network that ameliorates alpha-synuclein toxicity. *Science* (Co-submission with this work).
25. Haynes CM, Caldwell S, Cooper AA. An HRD/DER-independent ER quality control mechanism involves Rsp5p-dependent ubiquitination and ER-Golgi transport. *J Cell Biol*. 2002; 158:91–101. [PubMed: 12105183]
26. Donovan P, Poronnik P. Nedd4 and Nedd4-2: Ubiquitin ligases at work in the neuron. *Int J Biochem Cell Biol*. 2012:1–5.
27. Elden AC, et al. Ataxin-2 intermediate-length polyglutamine expansions are associated with increased risk for ALS. *Nature*. 2010; 466:1069–1075. [PubMed: 20740007]
28. Treusch S, et al. Functional links between A $\beta$  toxicity, endocytic trafficking, and Alzheimer's disease risk factors in yeast. *Science*. 2011; 334:1241–1245. [PubMed: 22033521]
29. Golbe LI, et al. Clinical genetic analysis of Parkinson's disease in the contursi kindred. *Ann Neurol*. 1996; 40:767–775. [PubMed: 8957018]
30. Muentner MD, et al. Hereditary form of parkinsonism--dementia. *Ann Neurol*. 1998; 43:768–781. [PubMed: 9629847]

31. Singleton AB, et al. alpha-Synuclein locus triplication causes Parkinson's disease. *Science*. 2003; 302:841. [PubMed: 14593171]
32. Waters CH, Miller CA. Autosomal dominant Lewy body parkinsonism in a four-generation family. *Ann Neurol*. 1994; 35:59–64. [PubMed: 8285594]
33. Yeger-Lotem E, et al. Bridging high-throughput genetic and transcriptional data reveals cellular responses to alpha-synuclein toxicity. *Nat Genet*. 2009; 41:316–323. [PubMed: 19234470]
34. Soldner F, et al. Parkinson's disease patient-derived induced pluripotent stem cells free of viral reprogramming factors. *Cell*. 2009; 136:964–977. [PubMed: 19269371]
35. Kim J-E, et al. Investigating synapse formation and function using human pluripotent stem cell-derived neurons. 2011:1–6.
36. Chambers SM, et al. Highly efficient neural conversion of human ES and iPS cells by dual inhibition of SMAD signaling. *Nat Biotechnol*. 2009; 27:275–280. [PubMed: 19252484]
37. Shi Y, Kirwan P, Livesey FJ. Directed differentiation of human pluripotent stem cells to cerebral cortex neurons and neural networks. *Nat Protoc*. 2012; 7:1836–1846. [PubMed: 22976355]
38. Lim MH. Preparation of a copper-based fluorescent probe for nitric oxide and its use in mammalian cultured cells. *Nat Protoc*. 2007; 2:408–415. [PubMed: 17406602]
39. McQuade LE, et al. Visualization of nitric oxide production in the mouse main olfactory bulb by a cell-trappable copper(II) fluorescent probe. *Proc Natl Acad Sci USA*. 2010; 107:8525–8530. [PubMed: 20413724]
40. Pincus D, et al. BiP Binding to the ER-Stress Sensor Ire1 Tunes the Homeostatic Behavior of the Unfolded Protein Response. *PLoS Biol*. 2010; 8:e1000415. [PubMed: 20625545]

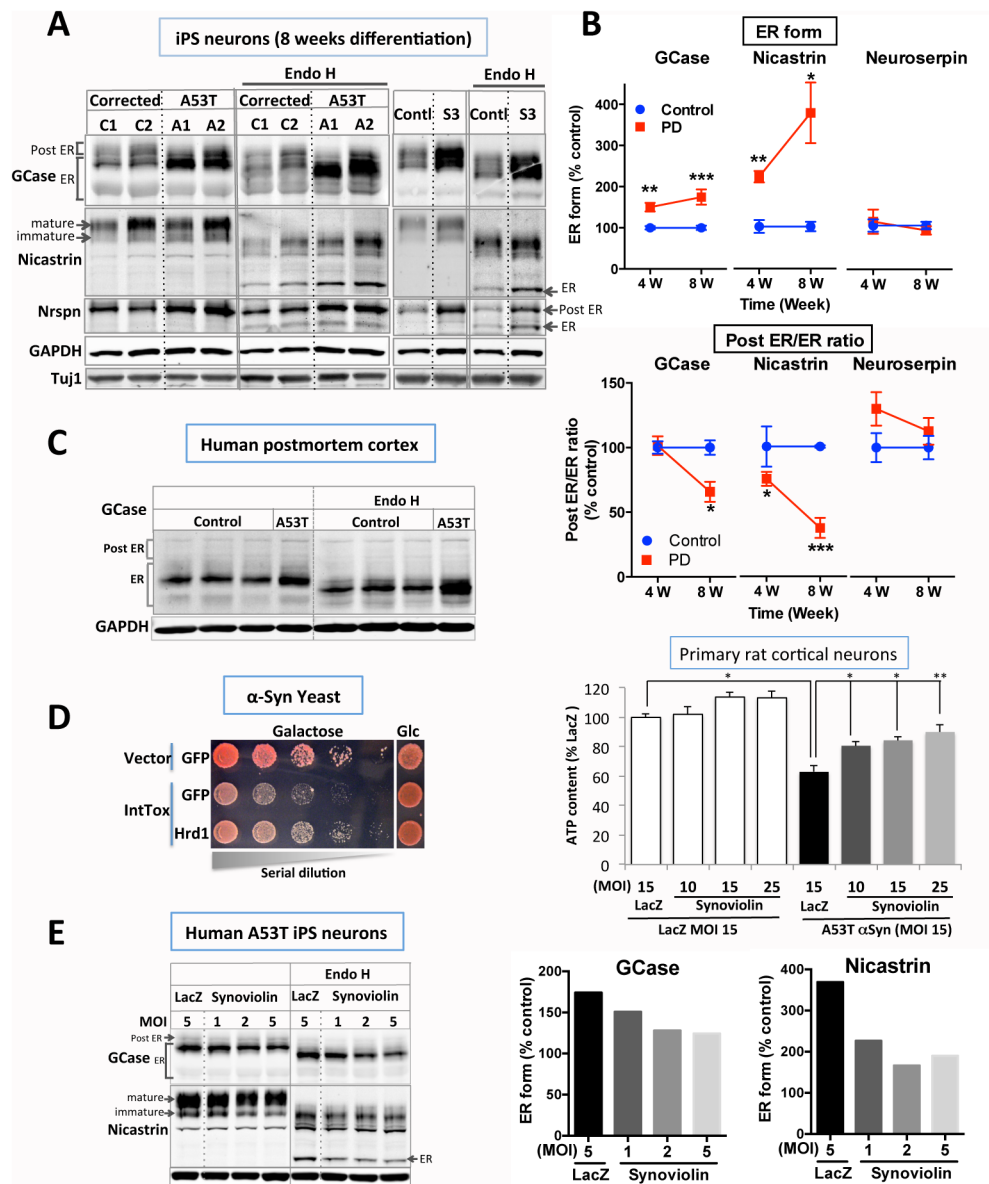


**Fig. 1.**

A specific link between  $\alpha$ Syn toxicity and nitrosative stress is identified in yeast (**A**) Fzf1 overexpression reduces  $\alpha$ Syn toxicity in yeast (IntTox) measured by growth of serially diluted yeast. (**B**) Protein nitration levels were measured by immunoblotting for 3-nitrotyrosine (3-NT). Strains expressing low (NoTox), intermediate (IntTox) and high (HiTox) levels of  $\alpha$ Syn were analyzed (11). Neurodegeneration-related models with equivalent toxicity (expressing A $\beta$  [ $\beta$ -amyloid peptide], Htt72Q [Huntingtin exon 1 with 72 glutamines] or Fus) were not similarly affected. (**C**) Fzf1 expression reduced  $\alpha$ Syn-induced increase in nitration. (**D and E**) NO-increasing deletion of Cox5A (  $\Delta$ Cox5A) increased protein nitration levels, whereas the NO-decreasing Cox5B deletion (  $\Delta$ Cox5B) reduced protein nitration levels (**D**). Toxicity was determined by propidium iodide stained cells using flow cytometry (**E**). Data represented as mean  $\pm$  SEM, \*\*\*,  $p < 0.001$  One way ANOVA with Bonferroni post-hoc test.

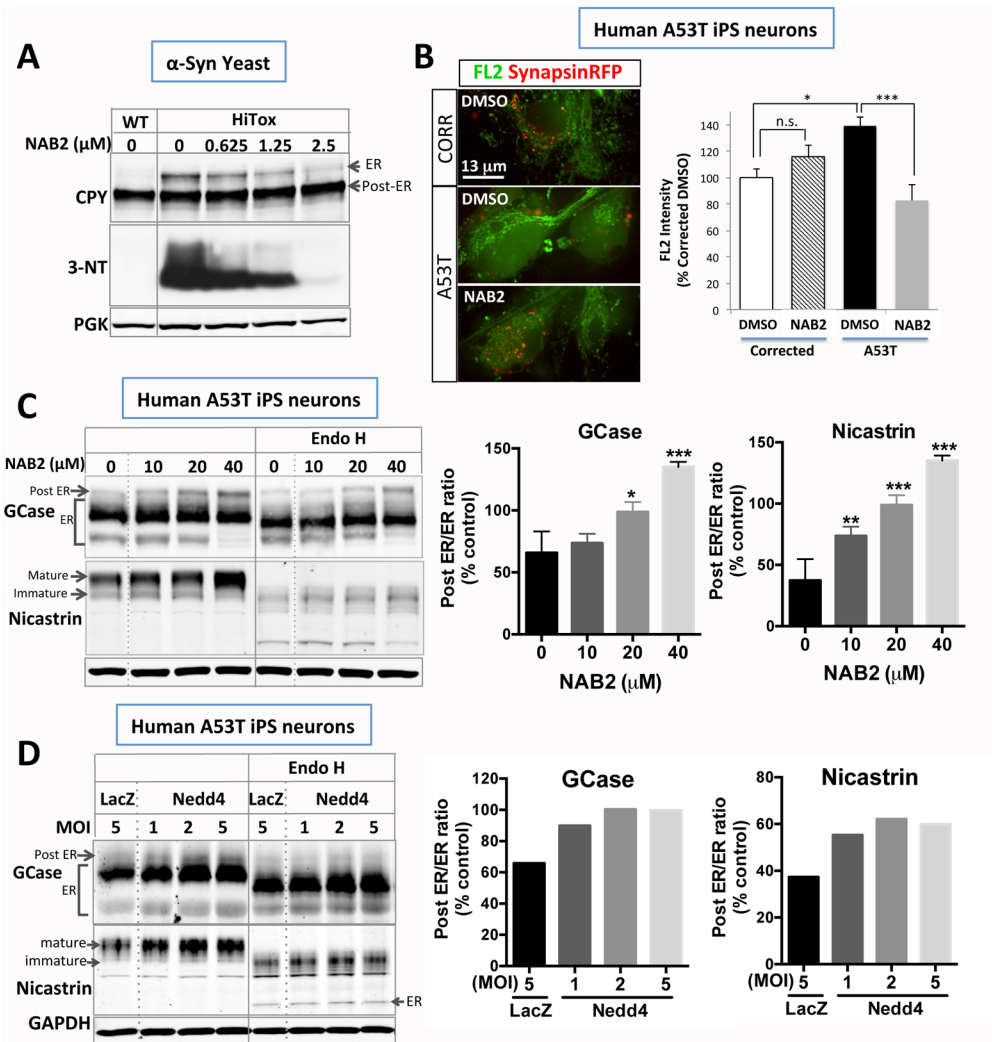


**Fig. 2.** Nitrosative stress is implicated in rat and human iPS neuron synucleinopathy models, and in the brain of a patient harboring the A53T  $\alpha$ Syn mutation. (A) Primary rat cortical cultures were infected with AAV2 mKate2 or A53T  $\alpha$ Syn-mKate2 (synapsin promoter). Cells were loaded with FL2 and live-imaged using a confocal microscope (neuronal soma: perforated circle). Perinuclear FL2 signal partially co-localized with ER tracker in rat neurons. (B–C) Increased NO (FL2) and 3-nitrotyrosine (3-NT) levels in human  $\alpha$ Syn<sup>A53T</sup> iPS neurons at 8 weeks. For the FL2 experiment (B), neural progenitors were transduced with lentivirus-RFP (synapsin promoter) to mark neurons. (D) Postmortem frontal cortex from a patient harboring A53T mutation exhibited increased 3-NT immunoreactivity. All data represented as mean  $\pm$  SEM, \*,  $p < 0.05$ , \*\*\*,  $p < 0.001$ , two tail t-test.



**Fig. 3.** Accumulation of ERAD substrates in patient cortical neurons is reversed by Synoviolin. (**A and B**) Cortical iPS neurons from  $\alpha$ Syn<sup>A53T</sup> (A1, A2),  $\alpha$ Syn<sup>corrected</sup> (C1, C2), a male human ES line (BGO1) and  $\alpha$ Syn<sup>triplication</sup> (S3) patients were harvested at 8–12 weeks. ER or post ER forms were distinguished based on sensitivity to Endoglycosidase H (Endo H) in GCase (glucocerebrosidase), Nicastrin and Nrspn (neuroserpin) (n=4~6, two tail t-test compared to control samples at each time point). (**C**) ER forms of GCase also accumulated in postmortem cortex from the A53T patient. (**D**) Co-expression of Hrd1 or its mammalian homolog, Synoviolin, reduced  $\alpha$ Syn toxicity in yeast and rat cortical neurons. Rat cultures were transduced by lentivirus encoding Synoviolin with varying multiplicity of infection (MOI) and co-transduced with lenti- $\alpha$ Syn<sup>A53T</sup> or lenti-LacZ. Cellular ATP content was measured (One way ANOVA with Bonferroni post-hoc test). (**E**) Lentiviral transduction of

Synoviolin reduced accumulation of ER forms of GCase and Nicastrin in  $\alpha$ Syn<sup>A53T</sup> iPS cortical neurons at 8–12 weeks. Baseline PD levels were equated to % control established in fig. 3 to depict biological significance of the change. All data represented as mean  $\pm$  SEM, \*;  $p < 0.05$ , \*\*;  $p < 0.01$ ; \*\*\*;  $p < 0.001$ ).

**Fig. 4.**

A small molecule modifier identified in an unbiased yeast screen and its target correct analogous defects in yeast and patient neurons. (A) NAB2 ameliorates  $\alpha$ Syn-induced ER accumulation of CPY and nitrosative stress in the yeast model. (B) NAB2 (5  $\mu$ M) decreases nitric oxide (FL2) levels in  $\alpha$ Syn<sup>A53T</sup> iPS neurons labeled with Synapsin-RFP. (C) NAB2 increases post-ER forms of and ameliorates the ER accumulation of GCase and Nicastrin in  $\alpha$ Syn<sup>A53T</sup> iPS neurons. (D) Lentiviral delivery of Nedd4 phenocopies the NAB2 treatment, increasing mature forms of GCase and Nicastrin. Baseline PD levels were equated to %control established in fig. 3. All data represented as mean  $\pm$  SEM (\*;  $p < 0.05$ , \*\*;  $p < 0.01$ , \*\*\*;  $p < 0.001$ , two tail t-test compared to control condition).